ISSN 1007-9327 (print)
ISSN 2219-2840 (online)

World Journal of *Gastroenterology*

World J Gastroenterol 2019 March 21; 25(11): 1289-1431

Published by Baishideng Publishing Group Inc

World Journal of Gastroenterology

Contents

Weekly Volume 25 Number 11 March 21, 2019

REVIEW

ORIGINAL ARTICLE

Basic Study

Case Control Study

Retrospective Study

Contents

World Journal of Gastroenterology

Volume 25 Number 11 March 21, 2019

ABOUT COVER

Editorial board member of *World Journal of Gastroenterology*, Jia-Xu Chen, MD, PhD, Professor, Traditional Chinese Medicine Diagnostics, School of Pre-Clinic Medicine, Beijing University of Chinese Medicine, Beijng 100029, China

AIMS AND SCOPE

World Journal of Gastroenterology (*World J Gastroenterol*, *WJG*, print ISSN 1007-9327, online ISSN 2219-2840, DOI: 10.3748) is a peer-reviewed open access journal. The *WJG* Editorial Board consists of 642 experts in gastroenterology and hepatology from 59 countries.

The primary task of *WJG* is to rapidly publish high-quality original articles, reviews, and commentaries in the fields of gastroenterology, hepatology, gastrointestinal endoscopy, gastrointestinal surgery, hepatobiliary surgery, gastrointestinal oncology, gastrointestinal radiation oncology, *etc*. The *WJG* is dedicated to become an influential and prestigious journal in gastroenterology and hepatology, to promote the development of above disciplines, and to improve the diagnostic and therapeutic skill and expertise of clinicians.

INDEXING/ABSTRACTING

The *WJG* is now indexed in Current Contents®/Clinical Medicine, Science Citation Index Expanded (also known as SciSearch®), Journal Citation Reports®, Index Medicus, MEDLINE, PubMed, PubMed Central, Scopus and Directory of Open Access Journals. The 2018 edition of Journal Citation Report® cites the 2017 impact factor for *WJG* as 3.300 (5-year impact factor: 3.387), ranking *WJG* as 35th among 80 journals in gastroenterology and hepatology (quartile in category Q2).

RESPONSIBLE EDITORS FOR THIS ISSUE

Responsible Electronic Editor: *Yan Huang* **Proofing Editorial Office Director:** *Ze-Mao Gong*

NAME OF JOURNAL
World Journal of Gastroenterology

ISSN
ISSN 1007-9327 (print) ISSN 2219-2840 (online)

LAUNCH DATE
October 1, 1995

FREQUENCY
Weekly

EDITORS-IN-CHIEF
Subrata Ghosh, Andrzej S Tarnawski

EDITORIAL BOARD MEMBERS
http://www.wjgnet.com/1007-9327/editorialboard.htm

EDITORIAL OFFICE
Ze-Mao Gong, Director

PUBLICATION DATE
March 21, 2019

INSTRUCTIONS TO AUTHORS
https://www.wjgnet.com/bpg/gerinfo/204

GUIDELINES FOR ETHICS DOCUMENTS
https://www.wjgnet.com/bpg/GerInfo/287

GUIDELINES FOR NON-NATIVE SPEAKERS OF ENGLISH
https://www.wjgnet.com/bpg/gerinfo/240

PUBLICATION MISCONDUCT
https://www.wjgnet.com/bpg/gerinfo/208

ARTICLE PROCESSING CHARGE
https://www.wjgnet.com/bpg/gerinfo/242

STEPS FOR SUBMITTING MANUSCRIPTS
https://www.wjgnet.com/bpg/GerInfo/239

ONLINE SUBMISSION
https://www.f6publishing.com

World Journal of Gastroenterology

Submit a Manuscript: https://www.f6publishing.com

World J Gastroenterol 2019 March 21; 25(11): 1366-1377

DOI: 10.3748/wjg.v25.i11.1366

ISSN 1007-9327 (print) ISSN 2219-2840 (online)

ORIGINAL ARTICLE

Case Control Study

Diffusion-weighted magnetic resonance imaging and micro-RNA in the diagnosis of hepatic fibrosis in chronic hepatitis C virus

Tarek Besheer, Hatem Elalfy, Mohamed Abd El-Maksoud, Ahmed Abd El-Razek, Saher Taman, Khaled Zalata, Wagdy Elkashef, Hossam Zaghloul, Heba Elshahawy, Doaa Raafat, Wafaa Elemshaty, Eman Elsayed, Abdel-Hady El-Gilany, Mahmoud El-Bendary

ORCID number: Tarek Besheer (0000-0002-0583-8860); Hatem Elalfy (0000-0002-5602-0989); Mohamed Abd El-Maksoud (0000-0002-7766-3684); Ahmed Abd El-Razek (0000-0002-9613-5932); Saher Taman (0002-5721-8508); Khaled Zalata (0000-0002-6678-7438); Wagdy Elkashef (0000-0003-2600-8003); Hosam Zaghloul (0000-0002-7201-1812); Heba Elshahawy (0000-0001-8521-876x); Doaa Raafat (0000-0001-6761-9826); Wafaa Elemshaty (0000-0002-2128-5901); Eman Elsayed (0000-0001-8924-3217); Abdel-Hady El-Gilany (0000-0001-9376-6985); Mahmoud El-Bendary (0000-0002-3751-5927).

Author contributions: Besheer T, Elalfy H, and El-Bendary M were involved in study conception and design; Abd El-Razek A and Taman S performed radiological imaging; Zaghloul H, Elshahawy H, Raafat D, Elemshaty W, and Elsayed E performed laboratory techniques; Zalata K and Elkashef W performed pathological diagnosis of the liver biopsies; El-Gilany AH and Abd El-Maksoud M acquired the data and performed analysis and interpretation of data; all authors were involved in the drafting and critical revision of the manuscript; all authors approved the final version of the manuscript.

Supported by Science and Technology Development

Tarek Besheer, Hatem Elalfy, Mohamed Abd El-Maksoud, Mahmoud El-Bendary, Department of Tropical Medicine and Hepatology, Mansoura Faculty of Medicine - Mansoura University, Mansoura 35111, Egypt

Ahmed Abd El-Razek, Saher Taman, Department of Diagnostic Radiology, Mansoura Faculty of Medicine - Mansoura University, Mansoura 35111, Egypt

Khaled Zalata, Wagdy Elkashef, Department of Pathology, Mansoura Faculty of Medicine - Mansoura University, Mansoura 35111, Egypt

Hossam Zaghloul, Heba Elshahawy, Doaa Raafat, Wafaa Elemshaty, Eman Elsayed, Department of Clinical Pathology, Mansoura Faculty of Medicine - Mansoura University, Mansoura 35111, Egypt

Abdel-Hady El-Gilany, Department of Public Health and Preventive Medicine, Mansoura Faculty of Medicine - Mansoura University, Mansoura 35111, Egypt

Corresponding author: Mahmoud El-Bendary, MD, Professor, Department of Tropical Medicine and Hepatology, Mansoura Faculty of Medicine - Mansoura University, Elgomhoria Street, Mansoura 35111, Dakahlia, Egypt. mm_elbendary@mans.edu.eg
Telephone: +20-1002592205
Fax: +20-502267016

Abstract

BACKGROUND

Diffusion-weighted magnetic resonance imaging has shown promise in the detection and quantification of hepatic fibrosis. In addition, the liver has numerous endogenous micro-RNAs (miRs) that play important roles in the regulation of biological processes such as cell proliferation and hepatic fibrosis.

AIM

To assess diffusion-weighted magnetic resonance imaging and miRs in diagnosing and staging hepatic fibrosis in patients with chronic hepatitis C.

METHODS

This prospective study included 208 patients and 82 age- and sex-matched controls who underwent diffusion-weighted magnetic resonance imaging of the abdomen, miR profiling, and liver biopsy. Pathological scoring was classified according to the METAVIR scoring system. The apparent diffusion coefficient

Foundation (STDF), Project NO. 3457 (TC/4/Health/2010/hep-1.6).

Institutional review board statement: The study protocol was reviewed and approved by the institutional ethics committee of the Mansoura Faculty of Medicine. (R.18.04.139.R1-2018/04/17).

Informed consent statement: Written informed consent was obtained from all eligible patients who were included in the study.

Conflict-of-interest statement: No conflict of interest.

Manuscript source: Invited manuscript

Received: November 12, 2018
Peer-review started: November 12, 2018
First decision: December 28, 2018
Revised: January 30, 2019
Accepted: February 15, 2019
Article in press: February 15, 2019
Published online: March 21, 2019

(ADC) and miR were calculated and correlated with pathological scoring.

RESULTS

The ADC value decreased significantly with the progression of fibrosis, from controls (F0) to patients with early fibrosis (F1 and F2) to those with late fibrosis (F3 and F4) (median 1.92, 1.53, and 1.25 × 10^{-3} mm^2/s, respectively) ($P = 0.001$). The cut-off ADC value used to differentiate patients from controls was 1.83 × 10^{-3} mm^2/s with an area under the curve (AUC) of 0.992. Combining ADC and miR-200b revealed the highest AUC (0.995) for differentiating patients from controls with an accuracy of 96.9%. The cut-off ADC used to differentiate early fibrosis from late fibrosis was 1.54 × 10^{-3} mm^2/s with an AUC of 0.866. The combination of ADC and miR-200b revealed the best AUC (0.925) for differentiating early fibrosis from late fibrosis with an accuracy of 80.2%. The ADC correlated with miR-200b ($r = - 0.61$, $P = 0.001$), miR-21 ($r = - 0.62$, $P = 0.001$), and miR-29 ($r = 0.52$, $P = 0.001$).

CONCLUSION

Combining ADC and miRs offers an alternative surrogate non-invasive diagnostic tool for diagnosing and staging hepatic fibrosis in patients with chronic hepatitis C.

Key words: Diffusion; Magnetic resonance imaging; Fibrosis; Liver; Hepatitis C virus; Micro-RNA

Core tip: We aimed to assess diffusion-weighted magnetic resonance imaging and micro-RNAs in diagnosis and staging of hepatic fibrosis. Patients underwent DWI of the abdomen, micro-RNA profiling, and liver biopsy. The apparent diffusion coefficient (ADC) and miR were calculated and correlated with METAVIR score. We found that ADC value was decreased from controls (F0) to patients with early fibrosis and those with late fibrosis. Combined ADC and miR-200b revealed the best result for differentiating early from late fibrosis and offer an alternative surrogate non-invasive diagnostic tool for diagnosis and staging of hepatic fibrosis in patients with chronic hepatitis C.

Citation: Besheer T, Elalfy H, Abd El-Maksoud M, Abd El-Razek A, Taman S, Zalata K, Elkashef W, Zaghloul H, Elshahawy H, Raafat D, Elemshaty W, Elsayed E, El-Gilany AH, El-Bendary M. Diffusion-weighted magnetic resonance imaging and micro-RNA in the diagnosis of hepatic fibrosis in chronic hepatitis C virus. *World J Gastroenterol* 2019; 25(11): 1366-1377
URL: https://www.wjgnet.com/1007-9327/full/v25/i11/1366.htm
DOI: https://dx.doi.org/10.3748/wjg.v25.i11.1366

INTRODUCTION

Hepatitis C virus (HCV) is responsible for chronic hepatic infection in 150-200 million people. Chronic liver disease results in the formation of fibrous tissue that impairs normal liver function, resulting in hepatic fibrosis, cirrhosis, portal hypertension, and hepatocellular carcinoma. Early detection of hepatic fibrosis has important therapeutic and prognostic implications for HCV-infected patients, since antiviral treatment can reduce hepatic decompensation and increase patient survival[1-5]. Liver biopsy is currently the gold standard for pathological assessment of hepatic fibrosis. However, it is an invasive maneuver with risks of complications such as hemorrhage, penetration to abdominal viscera, and pneumothorax and may result in death in 0.018% of patients; furthermore, the procedure is also prone to sampling error and observer variability[4-6]. Non-invasive diagnosis and staging of hepatic fibrosis is important for evaluating disease progression in patients with chronic liver diseases. Serum markers of liver fibrosis are widely available, but their results are variable[7-10]. Ultrasound elastography is used for grading hepatic fibrosis, but it is operator dependent[11-13]. Several magnetic resonance (MR) imaging sequences, such as

perfusion-weighted MR imaging, MR spectroscopy, MR elastography, and dynamic contrast-enhanced MR have the potential to provide quantitative information with variable diagnostic accuracy in the staging of liver fibrosis[13-15].

Micro-RNAs (miRs) are small noncoding RNA molecules that regulate gene expression at post-translational steps. The liver has numerous endogenous miRs that play important roles in the regulation of biological processes, such as cell proliferation and liver fibrosis. MiRs circulate in a cell-free form in body fluids including serum and are found mostly in exosomes and protein-RNA complexes. Several miRs were identified to be upregulated in serum in patients with chronic liver disease and liver fibrosis compared to those in healthy controls, and many of these were also correlated with the degree of liver fibrosis[16-19]. MiRNA-21 is upregulated at the onset of fibrosis in the human liver and may promote fibrogenic activation of fibroblasts. A considerable amount of evidence has shown that the miR-200 family participates in fibrosis. Moreover, a downregulation of circulating miR-29 is seen in patients with chronic liver injury and liver fibrosis. The level of miR-29 is correlated with the stage of liver fibrosis[18-21].

Diffusion represents the random Brownian motion of molecules, and MR imaging can detect signal changes caused by positional changes in molecules at this microscopic scale. The apparent diffusion coefficient (ADC) of the molecules measures the freedom of water proton diffusion in tissues and change according to the degree of cellularity of the lesion[22-26]. Diffusion-weighted MR imaging (DWI) is used for the assessment of liver fibrosis in adults and children[27-31]. The aim of the current study was to assess DWI and miRs in the diagnosis and staging of hepatic fibrosis in patients with chronic hepatitis virus C (CHC).

MATERIALS AND METHODS

Patients

The institutional review board approved this interventional study, and patients and controls provided written informed consent. The study assessed 215 consecutive patients with biopsy-proven CHC; patients were included if they had a histological diagnosis of CHC on a liver biopsy. HCV was defined by the presence of serum anti-HCV and HCV-RNA. Seven patients were excluded from our study due to the presence of hepatocellular carcinoma (n = 3), cardiac cirrhosis (n = 2), and hepatic metastasis (n = 2). The final number of patients was 208 (129 male and 79 female), and the median age was 36.3 ± 9.3 years. Eighty-two age- and sex-matched volunteers (47 male and 35 female) underwent MR imaging for reasons other than abdominal abnormalities; the median age was 38.3 ± 10.2 years. The patients and controls included in the study underwent DWI of the abdomen, miR tests, and liver biopsy from October 2012 to December 2015.

Routine magnetic resonance imaging

MR examinations were performed for all patients and controls using a T1.5 Tesla MR unit (Ingenia, Philips Best, Netherlands) using a bipolar diffusion encoding gradient. A 16-channel anterior phased array torso surface coil (dStream Torso coil) with a posterior body coil embedded in the table (dStream Total Spine coil) was applied. Routine axial T1-weighted images (TR/TE = 500/20 ms) and T2-weighted images (TR/TE = 6000/80 ms) were obtained.

Diffusion-weighted magnetic resonance imaging

Axial diffusion-weighted MR imaging of the liver was performed using free breathing spin echo planar sequence of echo planar imaging (EPI) readout. Automatic multi-angle projection shim and the chemical shift selective fat-suppression technique were applied. The motion probing gradient was applied before and after the 180 pulse with EPI readout. The b values applied were 0, 400, and 800 s/mm^2. The applied parameters were TR of 2800 ms, TE of 74 ms, EPI factor of 102, FOV of 25 cm × 25 cm, section thickness of 7 mm, interslice gap of 20%, acquisition matrix of 192 × 154, and number of excitations of six. After acquisition of the diffusion-weighted sequence, we obtained a set of images corresponding to each b-value applied. The ADC map was automatically calculated from the data set obtained at three b-values by commercially available software. The data acquisition time for the diffusion-weighted MR images was 1 min.

Image analysis

Image analysis was performed by a radiology expert in MR imaging with 25 years of experience (AA). Quantitative analysis of the ADCs of hepatic parenchyma was performed. A circular region of interest measuring 3-4 cm^2 was placed on the ADC

map at three different regions of hepatic parenchyma, on three consecutive slices away from the biliary and vascular structures, and more than 2 cm from the surface of the liver (Figure 1). The ADC value was calculated according to the following formula: ADC = -(lnSb2 - lnSb1)/(b2 -b1), where ln is the natural log, and Sb1 and Sb2 are the signal intensities in the region of interest placed on sections corresponding to the two different *b*-values (b1 and b2)[26]. The ADC value was automatically calculated in × 10^{-3} mm^2/s. The mean of these nine values was calculated and represents the final ADC value per subject used for statistical analysis.

Serum micro-RNAs assay

Blood samples were collected for the serum miRs assay just prior biopsy, and miR-200b, miR-21, and miR-29b were measured for all patients and control groups. Total RNA was extracted using a miRNeasy serum/plasma extraction kit (Qiagen, Valencia, CA, United States) using QIAzol lysis reagent according to the manufacturer's instructions. RNA quality was determined using a NanoDrop 2000 (Thermo Scientific, Waltham, MA, United States). Reverse transcription (RT) was carried out on 100 ng of total RNA in RT reactions in a final volume of 20 μL (incubated for 60 min at 37 °C and 5 min at 95 °C) using a miScript II RT Kit (Qiagen) according to the manufacturer's instructions. Serum expression levels of mature miRNAs, miR-200b, miR-29b, and miR-21, were evaluated using miScript miRNA PCR primer assays and a miScript SYBER green PCR kit (Qiagen) according to the manufacturer's protocol. The housekeeping miRNA SNORD68 was used as the internal control.

Liver biopsy

Percutaneous liver biopsy was performed by a hepatology expert in liver biopsy with 20 years of experience (BT). The biopsy was conducted at least 60 d before imaging to avoid misinterpretation attributed to early post-biopsy changes. The length of the specimen was not less than 1.2 cm (contained at least 10 portal tracts) that was fixed in formalin, put in paraffin, and stained with special stain according to the international criteria for pathological analysis. According to METAVIR score, hepatic fibrosis staging were classified as F0, no fibrosis; F1, portal fibrosis without septa; F2, portal fibrosis with few septa; F3, numerous septa without cirrhosis; and F4, cirrhosis[32].

Statistical analysis

Statistical analysis of the data was performed by Statistical Package for Social Science version 20 (SPSS Inc., Armonk, NY, United States). The data were presented as the mean and standard deviation (SD). The Kolmogorov-Smirnov test was performed to assess the normality of the data distribution. All data were revealed to be non-parametric. To compare two groups, Student's *t*-test was used. To compare more than two groups, one-way analysis of variance was used. Receiver operating characteristic (ROC) curves were used to determine the cut-off points of ADC, miR that were used to differentiate patients from controls, and early from late fibrosis with calculation of the area under the curve (AUC), accuracy, sensitivity, and specificity. The *P* value was considered significant if ≤ 0.05 at the 95% confidence interval. A multivariate logistic regression model was performed to determine the combination of parameters with the highest accuracy for differentiating controls from patients and early from late fibrosis. The Spearman correlation test was used to correlate the ADC with miRs.

RESULTS

Table 1 reveals the characteristics of patients and controls. The patients were divided into an early fibrosis group (F1 and F2) (*n* = 112, 38.6%) and a late fibrosis group (F3 and F4) (*n* = 96, 33.1%) along with a control group (F0) (*n* = 82, 28.3%). No significant differences in age and sex were found between patients and controls or between patients with early versus late fibrosis.

Table 2 shows the median ADC and miR values of patients versus controls. The median ADC values of patients (1.43 ± 0.22 × 10^{-3} mm^2/s) were significantly different (*P* = 0.001) compared with those of controls (1.92 ± 0.08 × 10^{-3} mm^2/s). The median miRNA values of patients were significantly different (*P* = 0.001) compared with those of controls.

Table 3 shows the ROC curve results with cut-off values of ADC and serum markers of patients and controls. The cut-off point of ADC values for differentiating patients from controls (Figure 2A) was 1.83 × 10^{-3} mm^2/s with an AUC of 0.992, accuracy of 97.1%, sensitivity of 98.6%, and specificity of 97%. The cut-off points of miR-200b, miR-21, and miR-29b used to differentiate patients from controls were 1.65, 1.35, and 0.91 with AUCs of 0.925, 0.865, and 0.937, respectively. The combination of

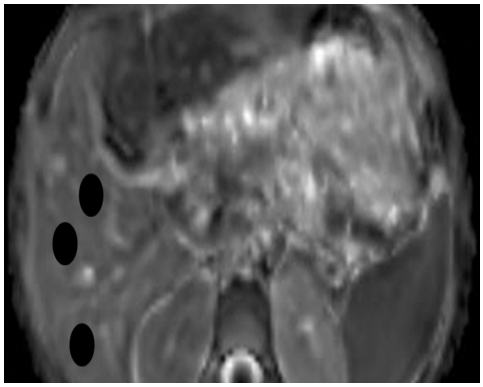

Figure 1 Regions of interest. Apparent diffusion coefficient map of the liver with locations of the regions of interest within the liver parenchyma.

ADC and miR-200 (Figure 2B) revealed an AUC of 0.995, accuracy of 96.9%, sensitivity of 100%, and specificity of 96%. ADC and miR-21 combined revealed an AUC of 0.992, accuracy of 96.2%, sensitivity of 100%, and specificity of 95%. The combination of ADC and miR-29b revealed an AUC of 0.992, accuracy of 95.9%, sensitivity of 100%, and specificity of 96%.

Table 4 shows the median, minimum, and maximum of ADC and serum markers of patients with early and late fibrosis. In differentiating the early fibrosis group from the late fibrosis, the median ADC value of early fibrosis ($1.5 \pm 0.2 \times 10^{-3}$ mm^2/s) was significantly ($P = 0.001$) different than that of late fibrosis ($1.25 \pm 0.17 \times 10^{-3}$ mm^2/s). The median values of miRNA-200b, miRNA-21, and miRNA-29b of early fibrosis were 3.4 ± 1.7, 1.9 ± 0.7, and 0.7 ± 0.2, respectively, and those of late fibrosis were 10.2 ± 4.8, 3.6 ± 1.2, and 0.4 ± 0.2, respectively; these values were significantly different ($P = 0.001$) between the groups.

Table 5 shows the cut-off values of ADC and miRs used to differentiate early from late fibrosis with the areas under the ROC curves, specificity, sensitivity, and accuracy. The ADC cut-off point used to differentiate early from late fibrosis was 1.54×10^{-3} mm^2/sec (Figure 3A) with an AUC of 0.866, accuracy of 81.7%, sensitivity of 99%, and specificity of 67%. The cut-off points of miRNA-200b, miRNA-21, and miRNA-29b used to differentiate early from late fibrosis were 3.55, 2.39, and 0.71 with AUCs of 0.888, 0.877, and 0.832 and accuracy of 73.5%, 80.2%, and 73.0%, respectively. The combined ADC and miR values used for differentiating early from late fibrosis were as follows: First, ADC and miR-200b (Figure 3B) showed an AUC of 0.925, accuracy of 80.2%, sensitivity of 71.7%, and specificity of 97.2%. Combining ADC and miR-21 revealed an AUC of 0.88, accuracy of 83.2%, sensitivity of 72.3%, and specificity of 97.5%. The combination of ADC and miRNA-29b revealed an AUC of 0.879, accuracy of 85.1%, sensitivity of 74.0%, and specificity of 96.5% (Table 5).

The values for miR-200b and miR-21 in controls were significantly increased ($P = 0.001$) compared with those in patients with early fibrosis and patients with late fibrosis. The median values of miR-200b and miR-21 increased as fibrosis decreased, and the median values of miRNA-29b decreased significantly with increased fibrosis. The ADC values were highly correlated with serum expression of miR-200b ($r = - 0.61$, $P = 0.001$), miR-21 ($r = - 0.62$, $P = 0.001$), and miR-29b ($r = 0.52$, $P = 0.001$).

DISCUSSION

In this study, the ADC values of patients were significantly lower than those of controls. This observation may be attributed to fibrogenesis engaging a range of cell types and mediators with progressive deposition of extracellular matrix proteins, reducing the interstitial spaces and distorting normal hepatic architecture[2,3,5]. These changes are responsible for restricted diffusion with reduction in the ADC values in patients with hepatic fibrosis. However, the staging of liver fibrosis with diffusion-weighted MR imaging is still controversial[33-35].

In this work, the ADC values of patients with late fibrosis are lower than those with early fibrosis. Previous studies reported that the values of the ADC are significantly different at the different stages of liver fibrosis/cirrhosis[33,34]. On the other hand, other studies did not find an association between grading of fibrosis and the ADC values[35,36]. The results in our study may be explained by the increase of hepatic connective tissue with accumulation of collagen, fatty tissue, and inflammatory cells,

Table 1 Comparison of demographic and laboratory data in F0, early fibrosis, and late fibrosis groups

Parameter	Control, *n* = 82	Early fibrosis, *n* = 112	Late fibrosis, *n* = 96	*P* value
Age	38.3 ± 10.2	34.1 ± 8.9	41.4 ± 7.8[23]	0.001
Gender (M:F)	47:35	69:43	60:36	0.8
ALT	36.29 ± 17.24	52.00 ± 36.07[1]	57.17 ± 36.88[23]	0.001
AST	35.00 ± 15.71	49.00 ± 25.12[1]	58.00 ± 35.12[23]	0.001
Albumin	4.10 ± 0.45	4.20 ± 0.44	3.80 ± 0.69[23]	0.001
Bilirubin	0.88 ± 0.48	0.81 ± 0.26	1.02 ± 0.46[2]	0.001
PCR	95746 ± 10111	391000 ± 213876[1]	254500 ± 129314[23]	0.001
AFP	7.50 ± 1.57	5.01 ± 2.95[1]	10.47 ± 6.78[23]	0.001

[1]Significance between control and early;
[2]Significance between control and late;
[3]Significance between late and early. Data expressed as mean and standard deviation, F one way analysis of variance test was used for comparison between the three groups. Student's *t*-test was used to compare between each two groups. ALT: Alanine transaminase; AST: Aspartate transaminase; PCR: Polymerase chain reaction; AFP: Alpha-fetoprotein.

which may lead to restricted diffusion with low ADC values in patients with late fibrosis[4,5,37].

In recent decades, miRs have emerged as key regulators of gene expression[38]. Evidence is accumulating that miRs participate in the progression of liver fibrosis and regulation of hepatic stellate cell (HSC) proliferation/apoptosis[39]; in addition, they have been reported as biomarkers of liver cirrhosis by some previous studies[40]. In this study, the levels of the miRs (miR-200b, miR-21, miR-29b) used to differentiate between controls and patients and between patients with early fibrosis and those with late fibrosis (Tables 2 and 4) were significantly different, and strong positive correlations were found between ADC and levels of miR-200b and miR-21. In patients with hepatic fibrosis, several miRs were identified to be upregulated in serum when compared to those in controls, and many of these miRs were also correlated with the degree of liver fibrosis. Several studies have discussed the role of miRs in fibrogenesis, but its value is still controversial[41,42]. Previously, miR-21 has been suggested to be upregulated at the onset of fibrosis in the human liver, and it may promote fibrogenic activation of fibroblasts.

A possible explanation for elevated miR-21 levels in advanced fibrosis is that miR-21 may regulate transforming growth factor (TGF) β2[41] and has been shown to activate HSCs through PTEN/AKT or ERK1 signaling pathways[41,42]. Moreover, induction of maturation of primary miR-21 precursor into mature miR-21 occurs *via* TGF-β. Another study added that a significant increase in hepatic miR-21 expression is associated with mitogen-activated protein kinase 3 signaling and epithelial-mesenchymal transition in liver fibrosis[42,43].

A considerable amount of evidence has demonstrated that the miR-200 family participates in fibrosis[16-20]. Previous studies reported that these miRs were upregulated and that circulating miR-29 was downregulated in patients with chronic liver injury and liver fibrosis. Levels of miR-29 correlated with the stage of liver fibrosis[17-21]. In the current study, the levels of miR-29 used to differentiate between controls and patients with fibrosis and between patients with early and those with late fibrosis were significantly different, and the level of miR-29 was negatively correlated with the fibrosis score. MiR-29b interferes with the process of fibrogenesis *via* inhibition of HSC activation, production of type I collagen[44], and expression of extracellular matrix genes in HSCs through the TGF-β/SMAD-CTGF signaling network[19,45,46]. Overexpression of miR-29 weakens collagen and matrix deposition in HSCs through interfering with genes of fibrogenesis[46].

Few studies discuss the role of combining imaging parameters, such as ultrasound elastography, with laboratory biomarkers in the detection and staging of hepatic fibrosis, but the results of such assessments overlap[12,13]. In the current study, combining ADC and miRs (200b, 21 and 29b) increased the sensitivity, specificity, and accuracy for differentiating controls from patients with fibrosis. The combination of ADC with miR-200 increased the AUC for detection of hepatic fibrosis and differentiation of patients with early fibrosis from those with late fibrosis.

Regarding limitations of the current work: First, the small sample size limited the statistical power. Therefore, further studies are needed at a larger scale to confirm the results of this work. Second, the use of diffusion-weighted MR imaging may have

Table 2 The median apparent diffusion coefficient and micro-RNAs values of patients versus controls

Parameter	Fibrosis, *n* = 208	Control, *n* = 82	*P* value
ADC	1.43 ± 0.22	1.92 ± 0.08	0.001
miR-200b	4.61 ± 1.21	1.20 ± 0.81	0.001
miR-21	2.70 ± 1.30	1.29 ± 0.40	0.001
miR-29b	0.58 ± 0.26	0.98 ± 0.16	0.001

Data expressed as mean and standard deviation. Student's *t*-test was used. miR: Micro-RNAs; ADC: Apparent diffusion coefficient.

limited the conclusions of our findings. Further studies using recent diffusion modules such as diffusion kurtosis imaging and diffusion tensor imaging at 3-tesla will improve the quality of the results. Third, this study used regions of interest for localization, and further studies should be performed using advanced post-processing methods, such as machine learning and histogram analysis[47-50].

In conclusion, we demonstrated that combining ADC and miRs offers a new non-invasive method for diagnosis and staging of hepatic fibrosis in patients with chronic hepatitis C.

Table 3 The receiver operating characteristic curve results with cut-off values of apparent diffusion coefficient and serum markers for patients and controls

Parameter	AUC	Cut-off point	Sensitivity	Specificity	Accuracy
ADC	0.992	1.825	98.6%	97.0%	97.1%
miR-200b	0.925	1.65	92.3%	82.2%	91.2%
miR-21	0.865	1.35	82.2%	76.0%	84.2%
miR-29b	0.937	0.91	92.3%	81.7%	91.0%
ADC and miR-200b	0.995	-	100%	96.0%	96.9%
ADC and miR-21	0.992	-	100%	95.0%	96.2%
ADC and miR-29b	0.992	-	100%	95.9%	95.9%

ROC: Receiver operating characteristic curve; AUC: Area under the curve; miR: Micro-RNAs; ADC: Apparent diffusion coefficient.

Table 4 The median, minimum, and maximum values of apparent diffusion coefficient and serum markers of patients with early and late fibrosis

Variables	Early fibrosis, *n* = 112	Late fibrosis, *n* = 96	*P* value
ADC	1.5 ± 0.2 (1-1.9)	1.25 ± 0.17 (0.9-1.5)	0.001
miR-200b	3.43 ± 1.71 (1.0-1.4)	10.17 ± 4.81 (1-28.4)	0.001
miR-21	1.9 ± 0.7 (1.0-4.2)	3.6 ± 1.17 (1.0-6.34)	0.001
miR-29b	0.7 ± 0.12 (0.12-1.00)	0.4 ± 0.2 (0.07-1.00)	0.001

The data expressed as median and range. Mann-Whitney *u* test was used. ADC: Apparent diffusion coefficient; miR: Micro-RNAs.

Table 5 The cut-off values of apparent diffusion coefficient and micro-RNAs used to differentiate early from late fibrosis with areas under the receiver operating characteristic curves, sensitivity, specificity and accuracy

Parameter	AUC	Cut-off point	Sensitivity	Specificity	Accuracy
ADC	0.866	1.53	99.0%	67.0%	81.7%
miR-200b	0.888	3.55	90.6%	59.5%	73.5%
miR-21	0.877	2.38	91.7%	70.3%	80.2%
miR-29b	0.832	0.70	87.5%	60.7%	73%
ADC and miR-200b	0.925	-	71.7%	97.2%	80.2%
ADC and miR-21	0.88	-	72.3%	97.5%	83.2%
ADC and miR-29b	0.879	-	74%	96.5%	85.1%

AUC: Area under the curve; miR: Micro-RNAs; ADC: Apparent diffusion coefficient.

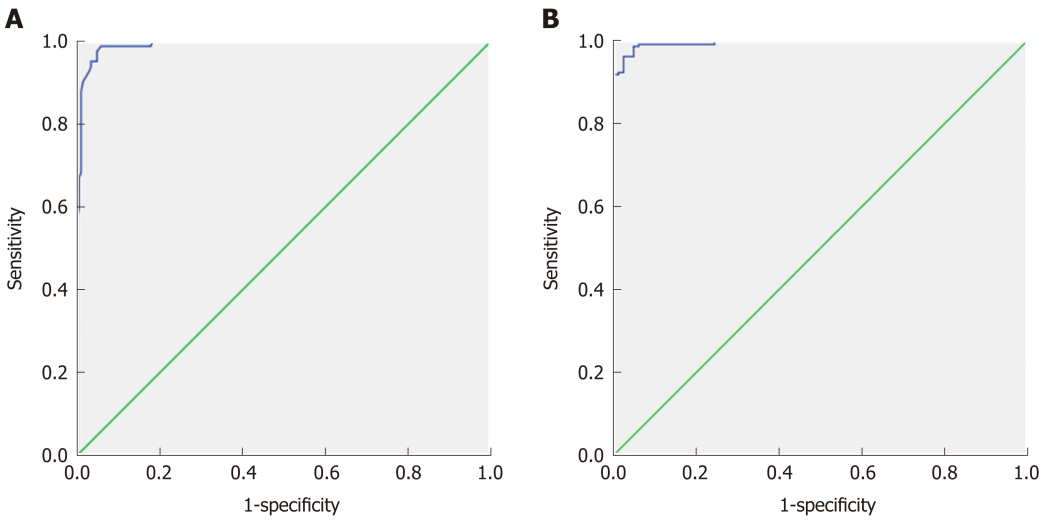

Figure 2 Receiver operating characteristic curve of patients *vs* controls. A: The cut-off apparent diffusion coefficient value used for differentiating patients from controls is 1.83 × 10^{-3} mm^2/s with an area under the curve of 0.992, sensitivity of 98.6%, and accuracy of 97.1%; B: The combination of apparent diffusion coefficient and miR-200b used for differentiating patients from controls shows an area under the curve of 0.995, sensitivity of 100%, and specificity of 96.9%.

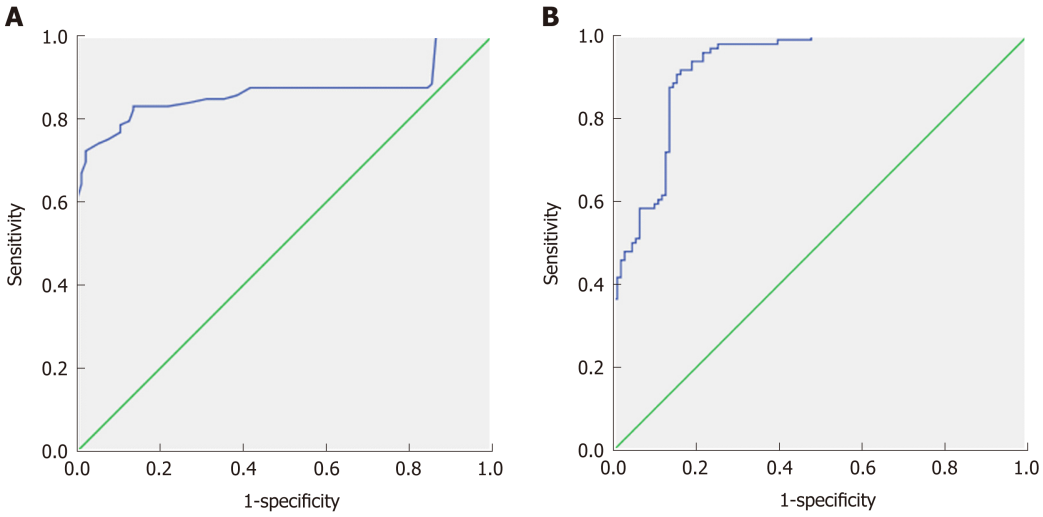

Figure 3 Receiver operating characteristic curve of early and late fibrosis. A: The cut-off apparent diffusion coefficient value for differentiating early from late fibrosis is 1.54 × 10^{-3} mm^2/s with an area under the curve of 0.866, sensitivity of 99.0% and accuracy of 81.7%; B: Combining apparent diffusion coefficient and miR-200b to differentiate early and late fibrosis patients shows an area under the curve of 0.925, sensitivity of 71.7% and accuracy of 80.2%.

ARTICLE HIGHLIGHTS

Research background

Hepatitis C virus infection is considered one of the most widespread causes of chronic liver disease that results in cirrhosis, fibrosis together with portal hypertension, and hepatocellular carcinoma. When it is possible to diagnose early hepatic fibrosis, the therapy will be more effective in the reduction of hepatic decompensation and improvement of patient survival. Liver biopsy is considered the gold standard for early detection of hepatic fibrosis, but it is invasive and has many side effects. Multiple non-invasive laboratory and imaging modalities could be used in detection and quantification of hepatic fibrosis but have variable accuracy. The liver contains multiple micro-RNAs (miR) (21, 200b and 29b) that have been correlated to the presence and degree of hepatic fibrosis. Magnetic resonance imaging (MRI) with diffusion-weighted imaging and apparent diffusion coefficient (ADC) can also detect and are correlated with hepatic fibrosis.

Research motivation

Early detection and staging of hepatic fibrosis are of great value in treatment of chronic liver disease caused by hepatitis C virus. The available methods to detect and stage fibrosis are either invasive (like biopsy) or non-invasive (like laboratory and imaging), which is not accurate. The combination of serum markers of hepatic fibrosis (miR 21, 200b and 29b) together with MRI with

diffusion-weighted imaging is a potential new dependable and non-invasive method to help in early detection and staging of hepatic fibrosis and cirrhosis.

Research objectives
In this prospective study, we evaluated the role of combining ADC and miR (21, 200b and 29b) as an alternative non-invasive tool for detection and staging of hepatic fibrosis in patients with chronic hepatitis C viral infection.

Research methods
From October 2012 to December 2015, 215 consecutive patients with histopathological evidence of chronic hepatitis C virus cirrhosis were included in our study. Seven cases were excluded, so the final number of the study patients was 208. Diffusion-weighted MRI (DWI) together with hepatitis C serum markers and serum miR (21, 200b and 29b) were performed for all patients. The MRI and laboratory results were compared with that of the control group containing 82 normal volunteers and with the results of liver biopsy histopathological examination.

Research results
In the current study, it was found that there was a significant decrease in ADC values in patients with early hepatic fibrosis and late fibrosis when compared to controls. Combining ADC results and miR data (200b, 21 and 29b) provided a highly sensitive, specific, and accurate tool to differentiate patients with hepatic fibrosis from normal control patients. This tool was best at differentiating patients from controls, with and accuracy of 96.9% and had an accuracy of 80.2% for differentiating early from late fibrosis.

Research conclusions
Combination of ADC and miR (21, 200b and 29b) is considered a safe, easy, and non-invasive tool in the detection and staging of hepatic fibrosis resulting from chronic hepatitis C viral infection.

Research perspectives
Combining imaging and laboratory results in detection and staging of hepatic fibrosis resulting from chronic hepatitis C virus infection is a valuable method because it is easy and non-invasive. However, a study with more patients will generate more accurate results. Also, use of advanced MRI machines with advanced post processing technology like diffusion tensor and diffusion kurtosis will improve the effectiveness and power of our findings.

REFERENCES

1 **Aydın MM**, Akçalı KC. Liver fibrosis. *Turk J Gastroenterol* 2018; **29**: 14-21 [PMID: 29391303 DOI: 10.5152/tjg.2018.17330]
2 **Hézode C**. Treatment of hepatitis C: Results in real life. *Liver Int* 2018; **38** Suppl 1: 21-27 [PMID: 29427481 DOI: 10.1111/liv.13638]
3 **Dolman GE**, Koffas A, Mason WS, Kennedy PT. Why, who and when to start treatment for chronic hepatitis B infection. *Curr Opin Virol* 2018; **30**: 39-47 [PMID: 29655092 DOI: 10.1016/j.coviro.2018.03.006]
4 **Besheer T**, El-Bendary M, Elalfy H, Abd El-Maksoud M, Salah M, Zalata K, Elkashef W, Elshahawy H, Raafat D, Elemshaty W, Almashad N, Zaghloul H, El-Gilany AH, Abdel Razek AA, Abd Elwahab M. Prediction of Fibrosis Progression Rate in Patients with Chronic Hepatitis C Genotype 4: Role of Cirrhosis Risk Score and Host Factors. *J Interferon Cytokine Res* 2017; **37**: 97-102 [PMID: 28068153 DOI: 10.1089/jir.2016.0111]
5 **Tapper EB**, Lok ASF. Use of Liver Imaging and Biopsy in Clinical Practice. *N Engl J Med* 2017; **377**: 2296-2297 [PMID: 29211669 DOI: 10.1056/NEJMc1712445]
6 **Gill US**, Pallett LJ, Kennedy PTF, Maini MK. Liver sampling: A vital window into HBV pathogenesis on the path to functional cure. *Gut* 2018; **67**: 767-775 [PMID: 29331944 DOI: 10.1136/gutjnl-2017-314873]
7 **Yang XZ**, Gen AW, Xian JC, Xiao L. Diagnostic value of various noninvasive indexes in the diagnosis of chronic hepatic fibrosis. *Eur Rev Med Pharmacol Sci* 2018; **22**: 479-485 [PMID: 29424906 DOI: 10.26355/eurrev_201801_14198]
8 **Trivedi HD**, Lin SC, T Y Lau D. Noninvasive Assessment of Fibrosis Regression in Hepatitis C Virus Sustained Virologic Responders. *Gastroenterol Hepatol (N Y)* 2017; **13**: 587-595 [PMID: 29391861]
9 **Attallah AM**, Abdallah SO, El Sayed AS, Omran MM, El-Bendary M, Farid K, Kadry M. Non-invasive predictive score of fibrosis stages in chronic hepatitis C patients based on epithelial membrane antigen in the blood in combination with routine laboratory markers. *Hepatol Res* 2011; **41**: 1075-1084 [PMID: 22035384 DOI: 10.1111/j.1872-034X.2011.00862.x]
10 **Attallah AM**, Omran MM, Farid K, El-Bendary M, Emran TM, Albannan MS, El-Dosoky I. Development of a novel score for liver fibrosis staging and comparison with eight simple laboratory scores in large numbers of HCV-monoinfected patients. *Clin Chim Acta* 2012; **413**: 1725-1730 [PMID: 22759976 DOI: 10.1016/j.cca.2012.06.031]
11 **Horowitz JM**, Venkatesh SK, Ehman RL, Jhaveri K, Kamath P, Ohliger MA, Samir AE, Silva AC, Taouli B, Torbenson MS, Wells ML, Yeh B, Miller FH. Evaluation of hepatic fibrosis: A review from the society of abdominal radiology disease focus panel. *Abdom Radiol (NY)* 2017; **42**: 2037-2053 [PMID: 28624924 DOI: 10.1007/s00261-017-1211-7]
12 **Barr RG**. Shear wave liver elastography. *Abdom Radiol (NY)* 2018; **43**: 800-807 [PMID: 29116341 DOI: 10.1007/s00261-017-1375-1]
13 **Kennedy P**, Wagner M, Castéra L, Hong CW, Johnson CL, Sirlin CB, Taouli B. Quantitative Elastography Methods in Liver Disease: Current Evidence and Future Directions. *Radiology* 2018; **286**: 738-763 [PMID: 29461949 DOI: 10.1148/radiol.2018170601]

14 **Petitclerc L**, Sebastiani G, Gilbert G, Cloutier G, Tang A. Liver fibrosis: Review of current imaging and MRI quantification techniques. *J Magn Reson Imaging* 2017; **45**: 1276-1295 [PMID: 27981751 DOI: 10.1002/jmri.25550]

15 **Berzigotti A**, França M, Martí-Aguado D, Martí-Bonmatí L. Imaging biomarkers in liver fibrosis. *Radiologia* 2018; **60**: 74-84 [PMID: 29108657 DOI: 10.1016/j.rx.2017.09.003]

16 **Almas I**, Afzal S, Idrees M, Ashraf MU, Amin I, Shahid M, Zahid K, Zahid S. Role of circulatory microRNAs in the pathogenesis of hepatitis C virus. *Virusdisease* 2017; **28**: 360-367 [PMID: 29291226 DOI: 10.1007/s13337-017-0407-3]

17 **Schueller F**, Roy S, Vucur M, Trautwein C, Luedde T, Roderburg C. The Role of miRNAs in the Pathophysiology of Liver Diseases and Toxicity. *Int J Mol Sci* 2018; **19**: pii: E261 [PMID: 29337905 DOI: 10.3390/ijms19010261]

18 **Piedade D**, Azevedo-Pereira JM. MicroRNAs, HIV and HCV: a complex relation towards pathology. *Rev Med Virol* 2016; **26**: 197-215 [PMID: 27059433 DOI: 10.1002/rmv.1881]

19 **Li Q**, Lowey B, Sodroski C, Krishnamurthy S, Alao H, Cha H, Chiu S, El-Diwany R, Ghany MG, Liang TJ. Cellular microRNA networks regulate host dependency of hepatitis C virus infection. *Nat Commun* 2017; **8**: 1789 [PMID: 29176620 DOI: 10.1038/s41467-017-01954-x]

20 **Shaker OG**, Senousy MA. Serum microRNAs as predictors for liver fibrosis staging in hepatitis C virus-associated chronic liver disease patients. *J Viral Hepat* 2017; **24**: 636-644 [PMID: 28211229 DOI: 10.1111/jvh.12696]

21 **Nakamura M**, Kanda T, Sasaki R, Haga Y, Jiang X, Wu S, Nakamoto S, Yokosuka O. MicroRNA-122 Inhibits the Production of Inflammatory Cytokines by Targeting the PKR Activator PACT in Human Hepatic Stellate Cells. *PLoS One* 2015; **10**: e0144295 [PMID: 26636761 DOI: 10.1371/journal.pone.0144295]

22 **Shenoy-Bhangle A**, Baliyan V, Kordbacheh H, Guimaraes AR, Kambadakone A. Diffusion weighted magnetic resonance imaging of liver: Principles, clinical applications and recent updates. *World J Hepatol* 2017; **9**: 1081-1091 [PMID: 28989564 DOI: 10.4254/wjh.v9.i26.1081]

23 **Culverwell AD**, Sheridan MB, Guthrie JA, Scarsbrook AF. Diffusion-weighted MRI of the liver-Interpretative pearls and pitfalls. *Clin Radiol* 2013; **68**: 406-414 [PMID: 22981728 DOI: 10.1016/j.crad.2012.08.008]

24 **Kanematsu M**, Goshima S, Watanabe H, Kondo H, Kawada H, Noda Y, Moriyama N. Diffusion/perfusion MR imaging of the liver: Practice, challenges, and future. *Magn Reson Med Sci* 2012; **11**: 151-161 [PMID: 23037559 DOI: 10.2463/mrms.11.151]

25 **Razek AA**. Diffusion magnetic resonance imaging of chest tumors. *Cancer Imaging* 2012; **12**: 452-463 [PMID: 23108223 DOI: 10.1102/1470-7330.2012.0041]

26 **Chandarana H**, Taouli B. Diffusion-weighted MRI and liver metastases. *Magn Reson Imaging Clin N Am* 2010; **18**: 451-464, x [PMID: 21094449 DOI: 10.1016/j.mric.2010.07.001]

27 **Razek AA**, Abdalla A, Omran E, Fathy A, Zalata K. Diagnosis and quantification of hepatic fibrosis in children with diffusion weighted MR imaging. *Eur J Radiol* 2011; **78**: 129-134 [PMID: 19926420 DOI: 10.1016/j.ejrad.2009.10.012]

28 **Hu XR**, Cui XN, Hu QT, Chen J. Value of MR diffusion imaging in hepatic fibrosis and its correlations with serum indices. *World J Gastroenterol* 2014; **20**: 7964-7970 [PMID: 24976733 DOI: 10.3748/wjg.v20.i24.7964]

29 **Razek AA**, Massoud SM, Azziz MR, El-Bendary MM, Zalata K, Motawea EM. Prediction of esophageal varices in cirrhotic patients with apparent diffusion coefficient of the spleen. *Abdom Imaging* 2015; **40**: 1465-1469 [PMID: 25732406 DOI: 10.1007/s00261-015-0391-2]

30 **Pasquinelli F**, Belli G, Mazzoni LN, Regini F, Nardi C, Grazioli L, Zignego AL, Colagrande S. MR-diffusion imaging in assessing chronic liver diseases: Does a clinical role exist? *Radiol Med* 2012; **117**: 242-253 [PMID: 22020423 DOI: 10.1007/s11547-011-0730-5]

31 **Leitão HS**, Doblas S, Garteiser P, d'Assignies G, Paradis V, Mouri F, Geraldes CF, Ronot M, Van Beers BE. Hepatic Fibrosis, Inflammation, and Steatosis: Influence on the MR Viscoelastic and Diffusion Parameters in Patients with Chronic Liver Disease. *Radiology* 2017; **283**: 98-107 [PMID: 27788034 DOI: 10.1148/radiol.2016151570]

32 **Bedossa P**, Poynard T. An algorithm for the grading of activity in chronic hepatitis C. The METAVIR Cooperative Study Group. *Hepatology* 1996; **24**: 289-293 [PMID: 8690394 DOI: 10.1002/hep.510240201]

33 **Bakan AA**, Inci E, Bakan S, Gokturk S, Cimilli T. Utility of diffusion-weighted imaging in the evaluation of liver fibrosis. *Eur Radiol* 2012; **22**: 682-687 [PMID: 21984447 DOI: 10.1007/s00330-011-2295-z]

34 **Sandrasegaran K**, Akisik FM, Lin C, Tahir B, Rajan J, Saxena R, Aisen AM. Value of diffusion-weighted MRI for assessing liver fibrosis and cirrhosis. *AJR Am J Roentgenol* 2009; **193**: 1556-1560 [PMID: 19933647 DOI: 10.2214/AJR.09.2436]

35 **Soylu A**, Kiliçkesmez O, Poturoğlu S, Dolapçioğlu C, Serez K, Sevindir I, Yaşar N, Akyildiz M, Kumbasar B. Utility of diffusion-weighted MRI for assessing liver fibrosis in patients with chronic active hepatitis. *Diagn Interv Radiol* 2010; **16**: 204-208 [PMID: 20658448 DOI: 10.4261/1305-3825.DIR.2810-09.1]

36 **Boulanger Y**, Amara M, Lepanto L, Beaudoin G, Nguyen BN, Allaire G, Poliquin M, Nicolet V. Diffusion-weighted MR imaging of the liver of hepatitis C patients. *NMR Biomed* 2003; **16**: 132-136 [PMID: 12884356 DOI: 10.1002/nbm.818]

37 **Do RK**, Chandarana H, Felker E, Hajdu CH, Babb JS, Kim D, Taouli B. Diagnosis of liver fibrosis and cirrhosis with diffusion-weighted imaging: Value of normalized apparent diffusion coefficient using the spleen as reference organ. *AJR Am J Roentgenol* 2010; **195**: 671-676 [PMID: 20729445 DOI: 10.2214/AJR.09.3448]

38 **Lambrecht J**, Mannaerts I, van Grunsven LA. The role of miRNAs in stress-responsive hepatic stellate cells during liver fibrosis. *Front Physiol* 2015; **6**: 209 [PMID: 26283969 DOI: 10.3389/fphys.2015.00209]

39 **Coll M**, El Taghdouini A, Perea L, Mannaerts I, Vila-Casadesús M, Blaya D, Rodrigo-Torres D, Affò S, Morales-Ibanez O, Graupera I, Lozano JJ, Najimi M, Sokal E, Lambrecht J, Ginès P, van Grunsven LA, Sancho-Bru P. Integrative miRNA and Gene Expression Profiling Analysis of Human Quiescent Hepatic Stellate Cells. *Sci Rep* 2015; **5**: 11549 [PMID: 26096707 DOI: 10.1038/srep11549]

40 **Krauskopf J**, de Kok TM, Schomaker SJ, Gosink M, Burt DA, Chandler P, Warner RL, Johnson KJ, Caiment F, Kleinjans JC, Aubrecht J. Serum microRNA signatures as "liquid biopsies" for interrogating hepatotoxic mechanisms and liver pathogenesis in human. *PLoS One* 2017; **12**: e0177928 [PMID: 28545106 DOI: 10.1371/journal.pone.0177928]

41 **Gabriely G**, Wurdinger T, Kesari S, Esau CC, Burchard J, Linsley PS, Krichevsky AM. MicroRNA 21

promotes glioma invasion by targeting matrix metalloproteinase regulators. *Mol Cell Biol* 2008; **28**: 5369-5380 [PMID: 18591254 DOI: 10.1128/MCB.00479-08]

42 **Zhao J**, Tang N, Wu K, Dai W, Ye C, Shi J, Zhang J, Ning B, Zeng X, Lin Y. MiR-21 simultaneously regulates ERK1 signaling in HSC activation and hepatocyte EMT in hepatic fibrosis. *PLoS One* 2014; **9**: e108005 [PMID: 25303175 DOI: 10.1371/journal.pone.0108005]

43 **Wei J**, Feng L, Li Z, Xu G, Fan X. MicroRNA-21 activates hepatic stellate cells via PTEN/Akt signaling. *Biomed Pharmacother* 2013; **67**: 387-392 [PMID: 23643356 DOI: 10.1016/j.biopha.2013.03.014]

44 **Huang YH**, Tiao MM, Huang LT, Chuang JH, Kuo KC, Yang YL, Wang FS. Activation of Mir-29a in Activated Hepatic Stellate Cells Modulates Its Profibrogenic Phenotype through Inhibition of Histone Deacetylases 4. *PLoS One* 2015; **10**: e0136453 [PMID: 26305546 DOI: 10.1371/journal.pone.0136453]

45 **Huang C**, Zheng JM, Cheng Q, Yu KK, Ling QX, Chen MQ, Li N. Serum microRNA-29 levels correlate with disease progression in patients with chronic hepatitis B virus infection. *J Dig Dis* 2014; **15**: 614-621 [PMID: 25138057 DOI: 10.1111/1751-2980.12185]

46 **Bandyopadhyay S**, Friedman RC, Marquez RT, Keck K, Kong B, Icardi MS, Brown KE, Burge CB, Schmidt WN, Wang Y, McCaffrey AP. Hepatitis C virus infection and hepatic stellate cell activation downregulate miR-29: MiR-29 overexpression reduces hepatitis C viral abundance in culture. *J Infect Dis* 2011; **203**: 1753-1762 [PMID: 21606534 DOI: 10.1093/infdis/jir186]

47 **França M**. Martí-Bonmatí L, Alberich-Bayarri Á, Oliveira P, Guimaraes S, Oliveira J, Amorim J, Gonzalez JS, Vizcaíno JR, Miranda HP. Evaluation of fibrosis and inflammation in diffuse liver diseases using intravoxel incoherent motion diffusion-weighted MR imaging. *Abdom Radiol (NY)* 2017; **42**: 468-477 [PMID: 27638516 DOI: 10.1007/s00261-016-0899-0]

48 **Razek AAKA**, Al-Adlany MAAA, Alhadidy AM, Atwa MA, Abdou NEA. Diffusion tensor imaging of the renal cortex in diabetic patients: Correlation with urinary and serum biomarkers. *Abdom Radiol (NY)* 2017; **42**: 1493-1500 [PMID: 28044190 DOI: 10.1007/s00261-016-1021-3]

49 **Seo N**, Chung YE, Park YN, Kim E, Hwang J, Kim MJ. Liver fibrosis: Stretched exponential model outperforms mono-exponential and bi-exponential models of diffusion-weighted MRI. *Eur Radiol* 2018; **28**: 2812-2822 [PMID: 29404771 DOI: 10.1007/s00330-017-5292-z]

50 **Razek AAKA**, Khashaba M, Abdalla A, Bayomy M, Barakat T. Apparent diffusion coefficient value of hepatic fibrosis and inflammation in children with chronic hepatitis. *Radiol Med* 2014; **119**: 903-909 [PMID: 24846081 DOI: 10.1007/s11547-014-0408-x]

P- Reviewer: El-Shabrawi MHF, Facciorusso A, McMillin MA, Wu C
S- Editor: Yan JP **L- Editor:** Filipodia **E- Editor:** Huang Y

Published By Baishideng Publishing Group Inc
7041 Koll Center Parkway, Suite 160, Pleasanton, CA 94566, USA
Telephone: +1-925-2238242
Fax: +1-925-2238243
E-mail: bpgoffice@wjgnet.com
Help Desk:http://www.f6publishing.com/helpdesk
http://www.wjgnet.com